Exact and approximate modeling of electrical properties of metal /insulator/semiconductor structures

Y. Khlifi[(1) (2)] , K. Kassmi[(1)], L. Roubi[(2)] , R. Maimouni[(1)]
[(1)] *Laboratoire d'Electronique Appliquée et d'Automatique (LEAA), Université Mohamed I[er], Faculté des Sciences, Dépt de Physique, Oujda, Maroc.*
[(2)] *Laboratoire de Physique du Solide (LPS), Université Mohamed I[er], Faculté des Sciences, Dépt de Physique, Oujda, Maroc.*

In this paper, we present the results of simulation concerning electrical properties of metal/insulator/ semiconductor structures both in the absence and presence of charge in the insulator. After establishing different basic equations in integral forms, we have given these equations analytically by using the Maxwell-Boltzmann approximation. Then, we have analyzed the potentials and electrical fields in the insulator and at the insulator-semiconductor interface in terms of the voltage applied to the structure and the charge density. This has yielded to the analysis of the relative errors made on these electrical parameters as a function of respectively the field in the insulator, the semiconductor doping and the charge density. The obtained results show a validation of the Maxwell-Boltzmann approximation, in particular for the electrical field determination in the structure (error is lower than 1.8%). The errors made by using this approximation are interpreted in term of semiconductor interface degeneracy.

PACS numbers : 70., 73.40.Qv

I. INTRODUCTION

Currently, the increasingly pushed integration of the integrated circuits, require a continuation of the research effort and development on the devices with thin films based on silicon. The elementary structure intervening in the majority of electronic components such as: transistors MOS, MOSFET or MISFET [1-4] and EEPROM memories [5,6] is the metal/insulator/semiconductor (MIS) structure where the insulator is made up either by the oxide (SiO_2) [7,8] or by the oxynitrure (SiOxNy) [9]. Currently, the reduction of dimension of these components implies on the one hand ultra-thin insulator thickness of about hundred Angströms or less, and on the other hand problems concerning the electrical properties of the structures such as: conduction [10-12] and destructive breakdown [10]. This is attributed qualitatively to a phenomena appearing in the thin insulating layer which are mainly: presence of defects [10,11] and storage of charges in the insulator[12-15],....

Previous works deals principally with modeling of MIS structures with relatively thick insulating layers (thickness higher than 150Å). However, few results relate to the modeling and the fine simulation of the electrical properties of the structure with thin insulating layers (thickness lower than 150Å). For the latter case, we show in this paper that the voltage drop across the semiconductor is no more negligible with respect to the potential drop across the insulator. Consequently, a detailed analysis is essential for modeling the electrical behavior of metal/ ultra-thin insulator/ semiconductor structures.

We present in this paper the basic equations, in integral and approximate forms, allowing the modeling of electrical properties of MIS structures in the absence and in the presence of charges in the insulator. Mainly, we analyze the results of simulation of the potential and the electrical field at the insulator/semiconductor interface in the semiconductor and in the insulator layer in terms of the voltage applied to the structure, the charge density and the semiconductor doping. Also, we study the validation of the various approximate models proposed.

II. MODELS OF ELECTRICAL PROPERTIES OF METAL/INSULATOR/SEMICONDUCTOR STRUCTURES

A. CARRIER DENSITIES IN A SEMICONDUCTOR, MAXWELL-BOLTZMANN APPROXIMATION

In a semiconductor, at the thermodynamic equilibrium (figure1), the carrier densities are calculated by summing up on all their energies the occupation probability and the state density which are function of semiconductor Fermi energy [14]:

$$n(x) = \frac{1}{2\pi^2}\left(\frac{2m_n^*}{\eta^2}\right)^{3/2} \int_{E_c}^{+\infty} fn(E)\,(E - E_c)^{1/2} dE \qquad (1)$$

$$p(x) = \frac{1}{2\pi^2}\left(\frac{2m_p^*}{\eta^2}\right)^{3/2} \int_{-\infty}^{E_V} fp(E)\,(E_V - E)^{1/2} dE \qquad (2)$$

Where m_n^* (m_p^*) is the free electron (hole) mass in the semiconductor, h(η) is the (reduced) Planck constant and E is the carrier energy in the semiconductor.
fn(E) and fp(E) are respectively the electron and hole occupation probability. They are given by the following expressions [16]:

$$fn(E) = \frac{1}{1 + \exp\left(\frac{E - E_{FS}}{kT}\right)} \quad (3)$$

$$fp(E) = \frac{1}{1 + \exp\left(-\frac{E - E_{FS}}{kT}\right)} \quad (4)$$

Where k is the Boltzmann constant and T is the Temperature (in our case is equal to 300°K).

By taking the potentials origin at the semiconductor bulk, let us denote:

$$\chi = \frac{E_V - E}{kT}, E_{FS} - E_v = q\Psi(x) - q\varphi_F + \frac{E_g}{2},$$

$$\upsilon = \varphi_F - \frac{Eg}{2q}.$$

$$\varepsilon = \frac{E - E_c}{kT}, E_c - E_{FS} = -q\Psi(x) + q\varphi_F + \frac{E_g}{2},$$

$$\eta = \frac{E_g}{2q} + \varphi_F, \beta = \frac{q}{kT}.$$

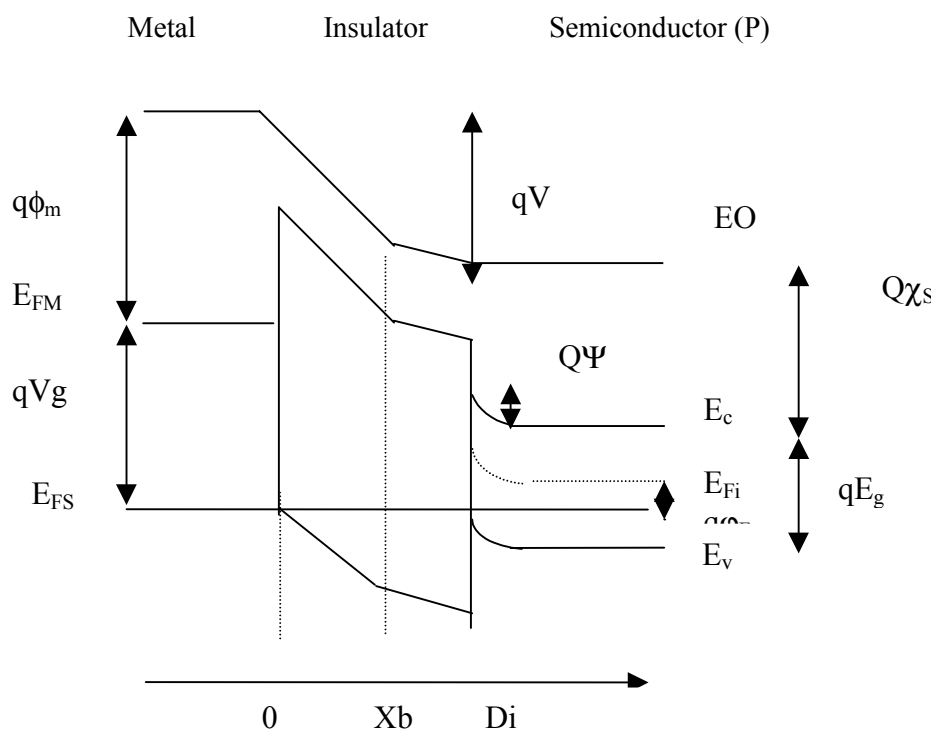

FIG. 1: Energy band diagram for MIS structure with negatively biased metal gate, in the presence of lamellate charge of density NT, located at the position Xb in the insulator

Where: E_{FM} : Metal Fermi level,
E_c : Energy level at the conduction band bottom,
E_v : Energy level at the highest valence band,
E_g : Band gap of the semiconductor,
φ_F : Energy difference between levels E_{Fi} and E_{FS},
Vg : The applied gate voltage,
χ_S : Semiconductor electron affinity,
Eo : Vacuum level,
E_{FS} : Semiconductor Fermi level.
E_{Fi} : semiconductor intrinsic Fermi level
Di : Insulator thickness,
φ_m : Metal workfunction.

Where q is the electronic charge ($1.6\ 10^{-19}$ c) and Ψ (x) is the potential as a function of the position x in the MIS structure.

We can deduce the electron n(x) and hole p(x) densities in integral forms:

$$n(x) = N_c F_{1/2}[\beta(-\eta + \Psi(x))] \quad (5)$$

$$p(x) = N_v F_{1/2}[\beta(\upsilon - \Psi(x))] \quad (6)$$

Where Nc is the effective electron state density in the conduction band and Nv is the effective hole state density in the valence band.

where:

$$F_{1/2}[\beta(-\eta+\Psi(x))] = \frac{2}{\sqrt{\pi}} \int_0^{+\infty} \frac{\varepsilon^{1/2}}{1+\exp(\varepsilon-\beta(\Psi(x)-\eta))}\, d\varepsilon \quad (7)$$

$$F_{1/2}[\beta(\upsilon-\Psi(x))] = \frac{2}{\sqrt{\pi}} \int_0^{+\infty} \frac{\chi^{1/2}}{1+\exp(\chi+\beta(\Psi(x)-\upsilon))}\, d\chi \quad (8)$$

When the Fermi energy E_{FS} is located in the band gap of the semiconductor, at least 3kT above the top of the valence band (E_v) or below the bottom of the conduction band (E_c), we can use the Maxwell-Boltzmann approximation which consists in neglecting in equations 3 and 4 the value of one with respect to the term in exponential [16]. Thus, the maximal errors on the occupation probabilities of the free carriers in the semiconductor are obtained for the electrons (holes) situated at the bottom (top) of the conduction (valence) band, and they are in order of 5%.

Nevertheless, if the Fermi energy E_{FS} is situated in the band gap at less than 3kT above the E_v or below the E_c, or when it is in the valence or conduction band at the insulator/ semiconductor interface, the interface region becomes decidedly degenerate, then the errors made on the occupation probabilities are high. The errors are even more high when the semiconductor degeneracy increases ($E_{FS} > E_c$ or $E_{FS} < E_v$). Therefore the errors made by using the Maxwell-Boltzmann approximation are more sensitive to the semiconductor degeneracy.

In the case of MIS structures, a charged zone appears at the semiconductor interface [16]. In this zone, the electrical potential $\Psi(x)$ depends on the position x (figure1). By taking into account the Maxwell-Boltzmann approximation, the densities n(x) and p(x) can be written, in terms of the potential $\Psi(x)$ and the carrier density in the semiconductor bulk (n_v, p_v), according to the approximate expressions:

$$n(x) \cong n_v \exp\left(\frac{q\Psi(x)}{kT}\right) \quad (9)$$

$$p(x) \cong p_v \exp\left(-\frac{q\Psi(x)}{kT}\right) \quad (10)$$

Where n_v (p_v) is the electron (hole) density in the semiconductor bulk.

Also n(x) and p(x) can be written, according to the Fermi energy level E_{FS}, in the following expressions [16]:

$$n(x) = n_i \exp\left(-\frac{E_c(x)-E_{FS}}{kT}\right) \quad (11)$$

$$p(x) = n_i \exp\left(\frac{E_v(x)-E_{FS}}{kT}\right) \quad (12)$$

Where n_i is the intrinsic density in the semiconductor, $E_c(x)$ is the energy level at the conduction band bottom as a function of position x inside the semiconductor, and $E_v(x)$ is the energy level at the highest valence band as a function of position x inside the semiconductor.

So, the conditions of the Maxwell-Boltzmann approximation are not always valid, this is particularly true at the insulator/ semiconductor interface. According to the applied voltage and charge density in the insulator, the semiconductor can be degenerated ($E_c(x) < E_{FS}$, or $E_{FS} < E_v(x)$). Consequently, the Maxwell-Boltzmann approximation can introduce a significant amount of errors. In the coming sections, we will analyze the influence of this degeneracy on the errors made on the various potentials and electrical fields in the MIS structure.

B. ELECTRICAL FIELD IN THE SEMICONDUCTOR

For the MIS structure and for a given bias voltage Vg, the electrical field E(x) in the semiconductor is given by the solution of the Poisson's equation. By taking the origin of the field in the semiconductor bulk, E(x) can be expressed in integral form [3,18]:

$$E(x) = \text{sign}(\Psi(x)) \left(\frac{2kT}{\varepsilon_o \varepsilon_s}\right)^{1/2} \left[\begin{array}{l} N_c \left\{F_{3/2}[\beta(-\eta+\Psi(x))] - F_{3/2}(-\beta\eta)\right\} \\ + N_v \left\{F_{3/2}[\beta(\upsilon-\Psi(x))] - F_{3/2}(\beta\upsilon)\right\} \\ + Ndop\ \beta\Psi(x) \end{array}\right]^{1/2} \quad (13)$$

Where ε_o is the permittivity of free space, ε_s is the semiconductor permittivity, Ndop is the semiconductor doping (in our case: Ndop = - NA, for P-type semiconductor).

The integral functions $F_{3/2}$ are given by:

$$F_{3/2}[\beta(-\eta+\Psi(x))] = \frac{4}{3\sqrt{\pi}} \int_0^{+\infty} \frac{\varepsilon^{3/2}}{1+\exp(\varepsilon-\beta(\Psi(x)-\eta))}\, d\varepsilon \quad (14)$$

$$F_{3/2}[\beta(\upsilon-\Psi(x))] = \frac{4}{3\sqrt{\pi}} \int_0^{+\infty} \frac{\chi^{3/2}}{1+\exp(\chi+\beta(\Psi(x)-\upsilon))}\, d\chi \quad (15)$$

At the semiconductor interface, the electrical field Es is deduced from equation 13 by taking $\Psi(x) = \Psi s$ (Ψs is the potential at the semiconductor interface (figure 1)).

From the equations (9,10) and Poisson's equation, we can easily deduce the approximate expression of the

electrical field E(x) in the semiconductor as a function of Ψ(x):

$$E(x) \cong \text{sign}\,(\Psi(x)) \left(\frac{2kT}{q L_{Di}}\right) \left[\exp\left(\frac{q\varphi_F}{kT}\right)\left(\exp\left(-\frac{q\Psi(x)}{kT}\right)+\frac{q\Psi(x)}{kT}-1\right) + \exp\left(-\frac{q\varphi_F}{kT}\right)\left(\exp\frac{q\Psi(x)}{kT}-1-\frac{q\Psi(x)}{kT}\right)\right]^{1/2} \quad (16)$$

Where L_{Di} is the intrinsic Debye length in the semiconductor, it is given by:

$$L_{Di} = \sqrt{\frac{2\,k\,T\varepsilon_o\,\varepsilon_s}{q^2\,n_i}} \quad (17)$$

Also, from the resolution of the Gauss equation at the insulator/semiconductor interface, we can deduce the approximate expression of the electrical field Ei in the insulator at the insulator/semiconductor interface:

$$Ei \cong \text{sign}(\Psi s)\frac{\varepsilon_o\,\varepsilon_s}{\varepsilon_o\,\varepsilon_i}\left(\frac{2\,k\,T}{q L_{Di}}\right) \left[\exp\left(\frac{q\varphi_F}{kT}\right)\left(\exp\left(-\frac{q\Psi s}{kT}\right)+\frac{q\Psi s}{kT}-1\right) + \exp\left(-\frac{q\varphi_F}{kT}\right)\left(\exp\frac{q\Psi s}{kT}-1-\frac{q\Psi s}{kT}\right)\right]^{1/2} \quad (18)$$

where : εi is the insulator permittivity.

C. ELECTRICAL FIELD AND POTENTIAL BARRIER IN THE INSULATOR

In the insulator, the expression of the potential barrier Ψ(x), where x vary from 0 (the position at the metal/insulator interface in the insulator) to Di^- (the position at the insulator/semiconductor interface in the insulator), is derived from the resolution of the Poisson's equation by taking $q\Psi(0)=q\varphi_m$ (figure1)[8]:

$$\Psi(x)=\Psi(0)-\frac{q}{\varepsilon o\,\varepsilon i}\int_0^x\left[\int_{x'}^{D_i^-}\rho(x'')\,dx''\right]dx'+E_i\,x \quad (19)$$

Where Ψ(0) is the potential at the metal/insulator interface in the insulator, and ρ (x) is the charge density in the insulator.
Considering:

$$E_i^*=\frac{\varnothing(D_i)-\varnothing(0)}{D_i}=\frac{V_i}{D_i} \quad (20)$$

Where Ψ(D_i) is the potential at the insulator/ semiconductor interface in the insulator, E_i^* is the fictive field in the insulator and V_i is the Voltage drop across the insulator.
Then we can deduce the expression, which links the fieldsEiand E_i^* :

$$E_i = E_i^* + \frac{q}{\varepsilon o\,\varepsilon i\,D_i}\int_0^{D_i^-}\left[\int_{x'}^{D_i^-}\rho(x'')\,dx''\right]dx' \quad (21)$$

Thus, knowing the fictive electrical field E_i^* or voltage drop V_i and the charge density ρ(x), we can deduce respectively the electrical field Ei and potential barrier distribution Ψ (x) in the insulator.

D. EQUIVALENT CHARGES AT THE INSULATOR/SEMICONDUCTOR INTERFACE

At the insulator/semiconductor interface, the electrical fields Es and E_i^* can be written using equation 21, by neglecting the interface states contribution [3], as:

$$\text{åòåsEs}-\text{åòåi}\left(\frac{V_i}{D_i}\right)=\frac{q}{D_i}\int_0^{D_i}\left[\int_{x'}^{D_i^-}\tilde{n}(x)'dx''\right]dx' \quad (22)$$

The right hand side of this equation is equivalent to a lamellate charge Q* located at the insulator/ semiconductor interface in the insulator. Thus, the fields Es and E_i^* are linked by an equation equivalent to that of Gauss, after having brought back all the charges stored in the insulator to the insulator/ semiconductor interface:

$$\varepsilon o\,\varepsilon s\,E_s-\varepsilon o\,\varepsilon i E_i^*=Q^* \quad (23)$$

Let us consider in the insulator a uniform voluminal density charge distribution. This distribution is equivalent to a lamellate charge [8], in the insulator, of density NT located at a position X_b of the metal / insulator interface (figure 1). The expression of the charge Q* can be written according to N_T and X_b in the form:

$$Q^*=q\,\frac{N_T\,X_b}{D_i} \quad (24)$$

This paper reports more quantitatively on the equivalent charge Q* influence on the various electrical parameters (Ψs, V_i, E_i, E_i^*,...). The influence of the lamellate charge in the insulator on the electrical properties of the MIS structures will be introduced in other work.
From figure 1, we can deduce the equation governing the applied voltage Vg, the potential surface Ψs, the fictive electrical field in the insulator E_i^* (or the electrical field Es) and the equivalent charge Q*:

$$Vg=\varphi m-\chi s-\frac{Eg}{2q}-\varphi_F+\Psi s+\frac{\left(\varepsilon o\,\varepsilon s\,Es-Q^*\right)}{\varepsilon o\,\varepsilon_i}D_i \quad (25)$$

Thus, for each voltage value Vg, we can deduce the potential surface Ψs, the electrical fields Es and E_i^* , and consequently E_i.

III. RESULTS OF SIMULATION & DISCUSSIONS

A. STEPS OF SIMULATION OF THE VARIOUS ELECTRICAL CHARACTERISTICS

The simulation of the various parameters is performed according to the following steps:

- Input the set of the parameters characterizing the structure (N_A, D_i, φ_m, N_T, X_b,...). With regard to the characteristics of the metal, we fixed the obtained values in the case of Chromium [10,18].
- Calculation of the various parameters and constants (Q*, flat band voltage,...).
- For each voltage value Vg, and by using the exact and approximate models, calculation of the field value Es from equation 25 by carrying out iterations on Ψs. When Ψs deviates from its exact value with an error lower than 10^{-5}, we obtain Ψs, Es and consequently V_i (or electrical field E_i^*).
- Storage of the results and plot of the various characteristics: Ψs (V_g), $E_s(V_g)$, E_i^* (V_g), $V_i(V_g)$...
- Calculations of the relative errors of each electrical parameter derived from the approximate equations.

B. SIMULATION OF POTENTIALS AND FIELDS OBTAINED BY THE EXACT MODELS

Figure 2 show typical variations of Es versus Vg. It appears that Es varies linearly with the applied voltage in the accumulation (negative bias) and inversion (positive bias) mode. On the other hand, Es is independent of the applied voltage in depletion (Vg close to zero).

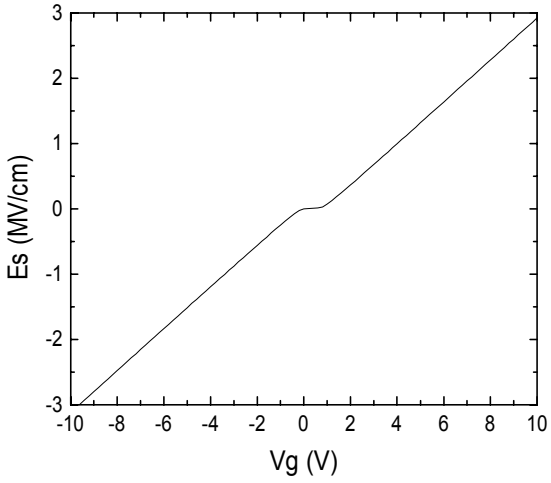

FIG.2 : Typical variation of Es versus Vg, in the absence of charge in the insulator.

In figure 3, we have plotted the ratio V_i/V_g versus the fictive electrical field E_i^* for various insulator thickness. The obtained curves show that in the case of thickness higher than 100Å the field in the insulator (Vi/Di) is roughly equal to V_g/D_i. In this case, the breakdown field (E_{BD}) (due to an abrupt and sharp decrease of the insulator resistivity) of the structure can be deduced directly from the applied voltage (E_{BD}=Vg/Di). However, for the thinner layers (thickness lower than 100Å) such an evaluation can involve considerable errors, the breakdown field is given by:

$$E_{BD}=\frac{V_i}{D_i} \qquad (26)$$

Consequently, the complete procedure of calculation of the electrical field Ei in the insulator is necessary .

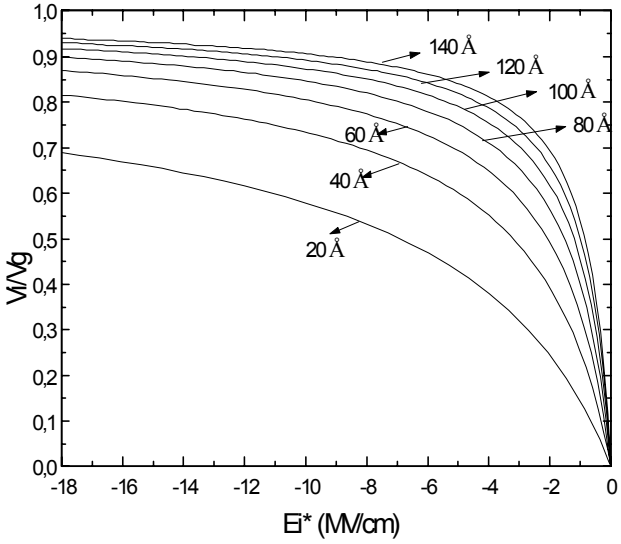

FIG. 3 : Vi/Vg ratio versus E_i^* : for insulator thickness ranging from 20Å to 140 Å, in the absence of charge in the insulator. Ndop =10^{15} cm^{-3}.

From the previous traces, we have plotted in figures 4 and 5, Ψs and Vi versus Vg for various charge densities NT. It is clear from these figures that there is a specific behavior depending on the applied voltage or the operating mode of the MIS structure:

- in depletion mode, Ψs increases in a significant way with V_g. However V_i, E_s and E_i^*, vary little with V_g.
- in accumulation or inversion mode, Ψ_s is less sensitive to the variations of the voltage Vg. On the other hand, the potential V_i , fields Es and E_i^* vary linearly with V_g.
- positive respectively negative charge causes a shift of the characteristics towards negative respectively positive voltage.

- the influence of the charge Q* is significant in depletion mode. On the other hand, in accumulation or inversion mode this influence is weak in particular on Vi and the various electrical fields in the structure.

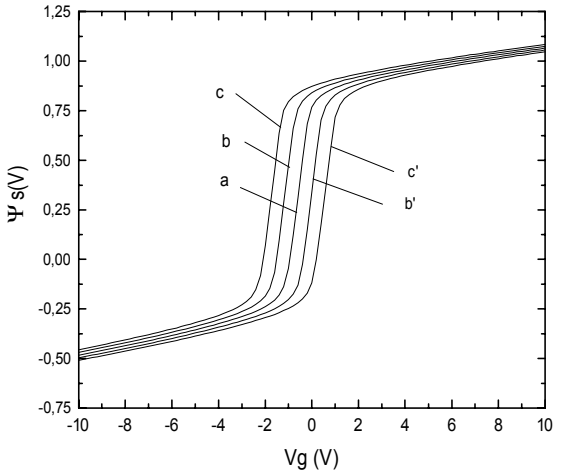

FIG. 4 : Variation of the semiconductor surface potential Ψs versus the applied voltage Vg.
Di = 100 Å, Ndop =10^{15} cm^{-3}, X_b=30Å,
N_T (cm^{-2}):
Positive charge: a) 0, b) 4 10^{12}, c) 8 10^{12},
Negative charge: a) 0, b') 4$10^{12}$, c') 8 10^{12}.

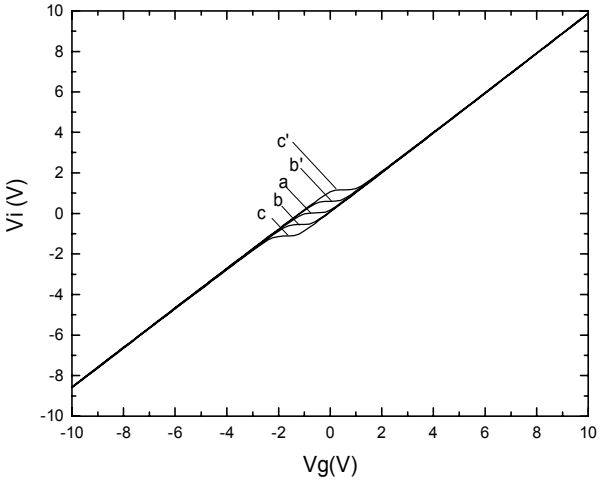

FIG. 5: Variation of the voltage drop Vi versus the applied voltage Vg and the charge density.
Di = 100 Å, Ndop =10^{15} cm^{-3}, X_b=30Å,
N_T (cm^{-2}):
Positive charge: a) 0, b) 4 10^{12}, c) 8 10^{12},
Negative charge: a) 0, b') 4$10^{12}$, c') 8 10^{12}.

C. SIMULATIONS OF POTENTIALS AND FIELDS OBTAINED BY THE APPROXIMATE MODELS IN THE STRUCTURE

As mentioned above, we have simulated the approximate models of potentials and fields in MIS structures according to the applied voltage V_g, the charge density NT and the semiconductor doping. By taking into account the previously obtained characteristics (exact calculations), we determined the relative errors made on the different parameters calculated from the approximate equations, in terms of E_i^* and the semiconductor doping.

C.1. ERRORS ON POTENTIAL AND ELECTRICAL FIELD IN THE STRUCTURE

In figures (6,7), we represented according to E_i^*, the relative errors on the semiconductor surface potential Ψs, potential V_i or fields (E_s, E_i or E_i^*) both in the presence and absence of the positive charge in the insulator. It appears that:

- in depletion mode, the error is negligible.
- in accumulation or inversion mode, the error increases with the electrical field E_i^*.
- in accumulation mode the error is significant compared to that in the inversion mode.
- in absence of a charge in the insulator, when the field E_i^* is about 18 MV/cm, the error can reach 45% (15%) in the accumulation (in the inversion) mode on the potential Ψs, and 1.6% (1%) on the potential Vi or the electrical fields in the structure.
- in the presence of the positive charge in the insulator, the errors on Ψs decrease by 2.5 % in accumulation and increase by 1.5 % in inversion. However, the errors on the various fields or potential Vi decrease (increase) by 0.2% in accumulation (in inversion). It should be noted that in the case of negative charges the same variations are obtained, but in opposite direction of that of positive charges
- at higher fields, the influence of the charge on the calculated errors on potential Vi or the various fields is negligible.

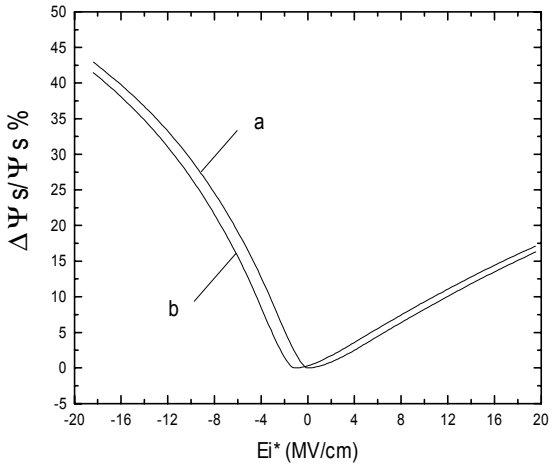

FIG. 6 : Influence of Ei* on the relative errors made on Ψs, in the absence and presence of positive charge in the insulator. Di = 100Å, Ndop =10^{15} cm^{-3},
X_b=30Å, N_T(cm^2): a) 0, b) 8$10^{12}$.

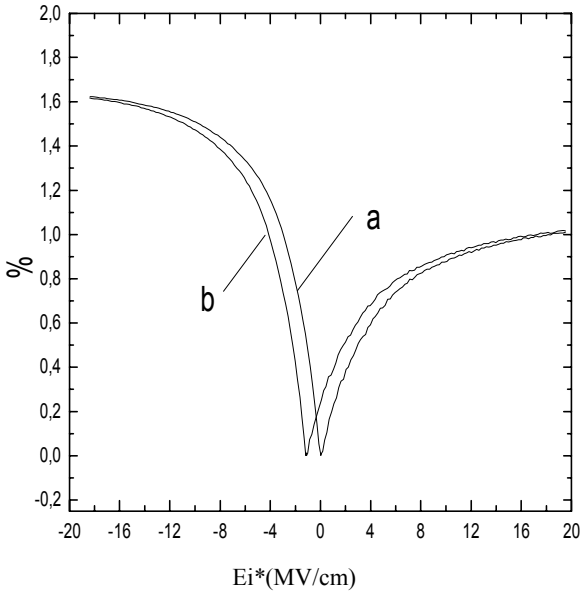

FIG. 7 : Influence of E_i^* on the relative errors made on Es, Ei*, Ei and Vi in the absence and presence of positive charge in the insulator.
Di = 100Å, Ndop =10^{15} cm^{-3}, X_b=30Å,
$N_T(cm^{-2})$: a) 0, b) 810^{12}.

To interpret these results, we have determined and plotted
in figure 8 energy differences (E_C - E_{FS})/kT and (E_{FS} - E_v)/kT at the semiconductor interface for each characteristic of figures 6 and 7. We deduce that the obtained errors are due to the semiconductor degeneracy: in accumulation (in inversion) mode the Fermi energy E_{FS} is located in the valence band (in the conduction band). In depletion mode the semiconductor is not degenerated (E_{FS} is located in the semiconductor band gap), consequently the various approximate equations can be used with practically negligible errors.

From figure 8 we deduce that the decrease (the increase) in errors (figures 6 and 7) in the accumulation (in the inversion) mode in the presence of positive charge, are due to the decrease (the increase) of the semiconductor interface degeneracy. In the case of negative charges, variations in opposite directions of that of the positive charges are obtained.

The increasing errors in the accumulation mode, compared to that in inversion (figures 6 and 7), is due to the strong semiconductor degeneracy in this mode.
Also, we have checked for a doping of about 10^{15} cm^{-3} that the semiconductor bulk is not degenerated: the Fermi energy E_{FS} is located in the semiconductor band gap at 9.3 kT above the top of the valence band and at 34 kT below the bottom of the conduction band.

By comparing the plots of figures 6 to 8, we deduce that the semiconductor degeneracy induces significant errors only on the semiconductor surface potential. On the other hand, the same degeneracy induce a weak errors (lower than 2%) on the voltage drop across the insulator Vi and on the fields in the semiconductor or insulator. Consequently, the approximate relations can be used to determine the various electrical fields in the MIS structures.

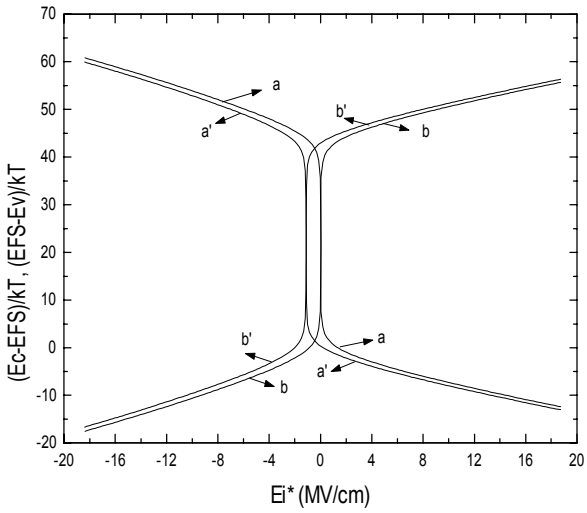

FIG. 8 : Energy differences (E_C -E_{FS})/kT (curves a and a') and (E_{FS} -E_v)/kT (curves b and b'), at the semiconductor interface, versus E_i^* in the absence (curves a and b) and presence of a positive charge (curves a' and b') in the insulator**.**
Di = 100Å, Ndop =10^{15} cm^{-3}, X_b=30Å, $N_T(cm^{-2})$: 8 10^{12}.

C.2. INFLUENCE OF THE SEMICONDUCTOR DOPING ON THE ERRORS MADE ON POTENTIALS AND ELECTRICAL FIELD IN THE STRUCTURE

Figure 9 shows the influence of semiconductor doping on the errors made on Ψs when the structure is polarized in inversion and accumulation mode, both in the absence and presence of charges in the insulator. We observe that these errors increase in the accumulation and can reach 60% for a doping value of about 10^{19} cm^{-3}. In the inversion, the errors decrease slightly with doping: when doping increases of about 7 decades, Ψs decreases by 5%. Also, the influence of the charges on the errors made on Ψs is independent of the semiconductor doping.

Concerning the influence of doping on the errors made on the voltage Vi and electrical fields (E_i^* , Ei, Es) in the structure, we found that they are independent of doping and are lower than 2 %.

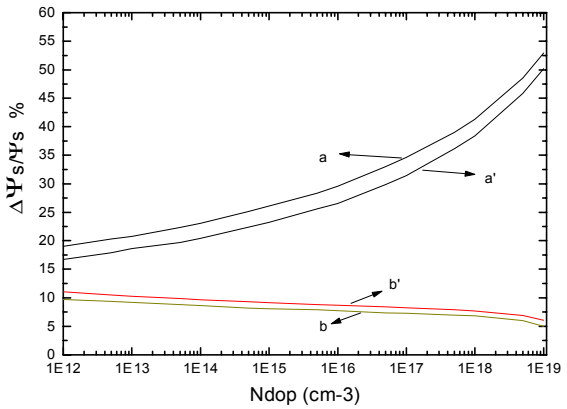

FIG. 9 : Relative errors made on Ψs versus semiconductor doping and the functioning mode of the MIS structure in the absence and presence of a positive charge in the insulator.
Di = 100 Å, Ei* (MV/cm): a) -10, a') -10, b) 10, b') 10,
(a), (b) : without charge,
(a'), (b'): with charge (Xb=30Å, N_T (cm^{-2}): 8 10^{12}).

As previously, we have plotted in figure 10, the energy differences $(E_C - E_{FS})/kT$ and $(E_{FS} - E_v)/kT$ versus the semiconductor doping for each characteristic of figure 9. It appears that they are sensitive to doping only for Ndop greater or equal to $10^{17}cm^{-3}$. From this value, the degeneracy increases (decreases) in the accumulation (in the inversion) mode and consequently the errors on the surface potential increase (decrease).

It should be noted that in the semiconductor bulk, the Fermi energy E_{FS} is always located in the semiconductor band gap for all the doping fixed in figure 9. When doping vary from 10^{12} cm^{-3} to 10^{19} cm^{-3}, this energy is located at 16.24 kT (27 kT) above the top of the valence band (below the bottom of the conduction band) for a doping of 10^{12} cm^{-3}, and at 0.12 kT (43.16 kT) above the top of the valence band (below the bottom of the conduction band) for a doping of 10^{19} cm^{-3}.

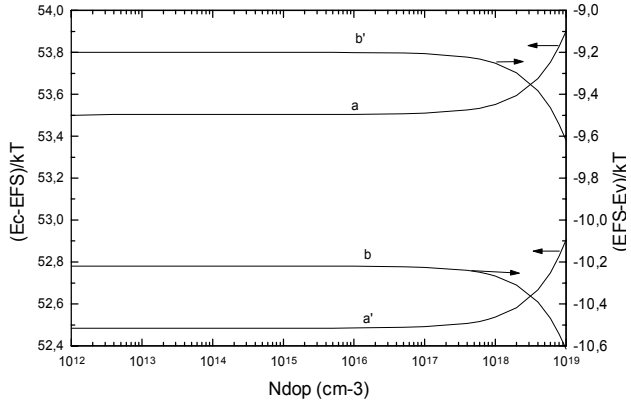

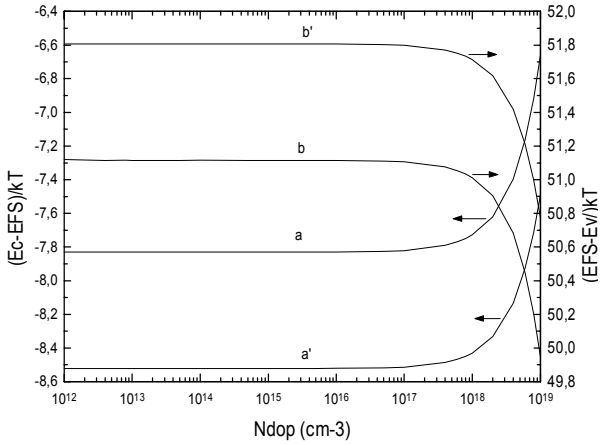

FIG. 10 : Energy differences $(E_C - E_{FS})/kT$ and $(E_{FS} - E_v)/kT$, at the semiconductor interface, versus the semiconductor doping.
Di = 100 Å, Ei*(MV/cm):
(A) -10, (B) 10
(a), (b) without charge in the insulator
(a'), (b') with charge in the insulator (X_b=30Å, N_T (cm^{-2}): 8 10^{12}).

IV. CONCLUSION

In this work, we have presented the basic equations in integral form, for the electrical properties of metal/insulator/semiconductor structure in the presence and absence of charges in the insulator. We showed that these charges are equivalent to a lamellate charge at the insulator/semiconductor interface. The numerical simulation of the potentials and electrical fields in the structure shows that the influence of the equivalent charge is significant in the depletion mode. In the inversion or accumulation mode the influence is negligible. We have established the analytical expressions of these equations by using the Maxwell-Boltzmann approximation. This approximation is well validated as shown by the results of simulation, particularly on the determination of the various electrical fields in the structure or the voltage drop across the insulator: the obtained errors are independent of doping and are about 1.6% (1%) in the accumulation (in the inversion) mode for a field in the insulator of about 18 MV/cm. However, the errors on the semiconductor surface potential depend of both effective field in the insulator and the semiconductor doping: they can reach 60% for a field of about 18 MV/cm and a doping of $10^{19}cm^{-3}$.

The increase (decreases) in the errors is attributed to the increase (decreases) of degeneracy at the semiconductor interface. This degeneracy is significant in the accumulation mode compared to that in the inversion mode, and increases with the semiconductor doping from a density which is about 10^{17} cm^{-3}.

Thus, in the metal/insulator/semiconductor structure the Maxwell-Boltzmann approximation is justified for the determination of the analytical expressions of the voltage drop in the insulator and the various electrical fields in the structure.

[1] W. Chen, A. Balasinski, B Zhang, T.P. MA, IEEE. Electron Device.Letters,Vol.**13**, n° 4, p. 201, April 1992

[2] K. Nagai, Y. Hayachi, Solid-State Electronics. vol. **33**, n°2, p. 223, 1990

[3] K.K. Hung, Y.C. Cheng, J. Appl. Phys.**59** (3), p. 816, 1986

[4] H. Hayama, W.I. Milne, Solid State Electronics vol. **33**, n°2, p. 279, 1990

[5] A. Coccannon, S. Keeney, A. Mathewson, R. Bez, C Lombardi, IEEE Transactions on Electron Devices. Vol. **40**, n°7, p. 1258, July 1993

[6] H. Fukuda, T. Hayashi, A. Uchiyama, T. Iwabuchi, Electr Letters, vol. **29**, n° 11, p. 947, May 1993

[7] G. Sarrabayrouse, J.L. Prom, K. Kassmi, IEE Proc, vol. **137**, Pt.G, N°6, p. 475, 1990

[8] K. Kassmi, Thesis of Paul Sabatier University. Toulouse, 904, 1991

[9] P. Temple Boyer, F Olivie, K. Kassmi, E. Scheid, G. Sarrabayrouse, A.Martinez, Solid state Electronics. Vol. **41**, N°7, p. 951, 1997

[10] K. Kassmi, J.L. Prom, G. Sarrabayrouse, Solid State. Electron, vol.**34**, p. 509, 1991

[11] P. Olivo, T.N. Nguyen, B Ricco, IEEE.Trans. Electron Devices ED-35, p. 2259, 1988

[12] D.J. Dumin, J.R. Cooper, J.R. Maddux, R. Scott, D.P. Wong, J. Appl. Phys.**76** (1), p. 319, 1 July 1994

[13] I.C.Chen, S.E. Holland, C. HU, Trans IEEE. Electron Devices, ED.32, 2, p. 413, 1985

[14] I.C. Chen, S. Holland, Chenming HU, IEEE Electron Device Letter, Vol. EDL-7, 3, p. 164, 1986

[15] M.S. Liang, S.H. Haddad, W. Cow, S. Cagnina, Iedm, p. 394, 1986

[16] S.M. SZE, Physics of semiconductors Devices, J. Wiley New York, 1981

[17] Y. Khlifi, K. Kassmi, L. Roubi, R. Maimouni, Mediterranean Conference on Electronics and Automatic (MCEA' 98), Marrakech (Morocco) 17-19 September

[18] S. Kar, W.E. Dahlke, Solid State electronics, **15**, p. 221, 1972